

# Jammed particulate systems are inherently nonharmonic

Carl F. Schreck<sup>1</sup>, Thibault Bertrand<sup>2</sup>, Corey S. O'Hern<sup>3,1</sup>, and M. D. Shattuck<sup>4</sup>

<sup>1</sup>*Department of Physics, Yale University, New Haven, Connecticut 06520-8120, USA*

<sup>2</sup>*Département Physique, Ecole Normale Supérieure de Cachan,  
61 Avenue du Président Wilson, 94235 Cachan, France*

<sup>3</sup>*Department of Mechanical Engineering and Materials Science,  
Yale University, New Haven, Connecticut 06520-8286, USA and*

<sup>4</sup>*Benjamin Levich Institute and Physics Department,*

*The City College of the City University of New York, New York, New York 10031, USA*

Jammed particulate systems, such as granular media, colloids, and foams, interact via one-sided forces that are nonzero only when particles overlap. We find that systems with one-sided repulsive interactions possess no linear response regime in the large system limit ( $N \rightarrow \infty$ ) for all pressures  $p$  (or compressions  $\Delta\phi$ ), and for all  $N$  near jamming onset  $p \rightarrow 0$ . We perform simulations on 2D frictionless bidisperse mechanically stable disk packings over a range of packing fractions  $\Delta\phi = \phi - \phi_J$  above jamming onset  $\phi_J$ . We apply perturbations with amplitude  $\delta$  to the packings along each eigen-direction from the dynamical matrix and determine whether the response of the system evolving at constant energy remains in the original eigenmode of the perturbation. For  $\delta > \delta_c$ , which we calculate analytically, a single contact breaks and fluctuations abruptly spread to all harmonic modes. As  $\delta$  increases further all discrete harmonic modes disappear into a continuous frequency band. We find that  $\langle \delta_c \rangle \sim \Delta\phi/N^\lambda$ , where  $1 > \lambda > 0.5$ , and thus jammed particulate systems are inherently nonharmonic with no linear vibrational response regime as  $N \rightarrow \infty$  over the full range of  $\Delta\phi$ , and as  $\Delta\phi \rightarrow 0$  at any  $N$ .

PACS numbers: 83.80.Fg, 63.50.-x, 62.30.+d, 61.43.-j

**Introduction** Granular materials, which are collections of macroscopic grains that interact via contact forces, such as sand, powders, pharmaceutical, and consumer products, display strongly nonlinear spatio-temporal dynamics even when they are weakly driven. In stark contrast to conventional solids [1] granular solids possess nonaffine, hysteretic, and time-dependent mechanical response [2], and dispersive, attenuated, and noisy acoustic response [3, 4] for micro-strains.

Crystalline and amorphous atomic and molecular solids display well-defined linear response regimes for small perturbations. Similarly, there has been a large research effort to identify linear response regimes for granular and other jammed particulate systems. Examples include effective medium theory [5] for granular media, which provides predictions for the elastic moduli as a function applied pressure, and approaches that assume the vibrational modes of static, mechanically stable (MS) packings obtained from the dynamical matrix in the harmonic approximation describe the mechanical response [6], vibrations [7, 8], and heat flow [9] of weakly perturbed and fluctuating particulate systems.

However, it has not been determined whether jammed particulate systems possess a linear response regime, and if so, over what range of perturbation amplitudes and timescales. To address this fundamental question for granular media, it is important to understand separately the manifold contributions to nonharmonicity including nonlinear, dissipative, and frictional particle interactions [10], inhomogeneous force propagation [11, 12], and breaking and forming of intergrain contacts [3]. Here, we describe computational studies to quantify perhaps the most important contribution to nonharmonicity in

jammed particulate media—the one-sided nature of contact interactions—interparticle forces are only nonzero when two grains are in contact, but are strictly zero when they are out of contact.

We find that one-sided interactions make jammed particulate materials *inherently* nonharmonic, *i.e.* nonharmonic even in the limit of vanishing perturbation amplitude, due to changes in the contact network following the perturbation [13]. Specifically, we employ the harmonic approximation and calculate the eigenmodes of the dynamical matrix [14] for MS frictionless packings, subject the packings to vibrations along the harmonic set of eigenmodes, and quantify the frequency content of the response versus the perturbation amplitude  $\delta$ . We find that systems become nonharmonic (*i.e.* the response is not confined to the original mode of excitation) when only a *single* contact is broken (or gained) at a critical  $\delta_c$  that depends on the original mode of excitation. For  $\delta > \delta_c$  the response first spreads to all (harmonic) eigenmodes with an amplitude that scales inversely with frequency, and then becomes continuous with an average frequency that decreases with  $\delta$ . We show that  $\langle \delta_c \rangle$  averaged over the modes of excitation tends to zero in the large system limit even for highly compressed systems, and tends to zero in the limit of zero compression at all system sizes. Thus, jammed particulate systems possess no harmonic regime in the large system limit and at jamming onset for any system size.

**Model and Simulations** We focus on frictionless MS packings of bidisperse disks in 2D with system sizes in the range  $N = 12$  to 1920 particles using periodic boundaries in square simulation cells ( $2N/3$  disks with diameter  $\sigma$  and  $N/3$  disks diameter  $1.4\sigma$ ). The disks interact via the

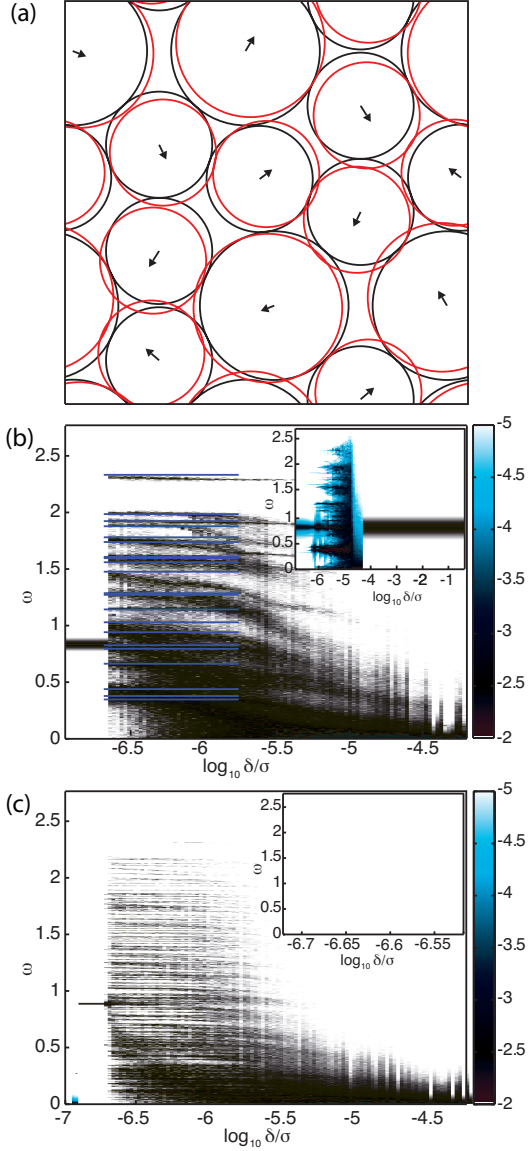


FIG. 1: (a) Mechanically stable (MS) packing of frictionless disks for  $N = 12$  at  $\Delta\phi = 10^{-5}$  (black solid) and a packing perturbed along the 6th eigenmode of the dynamical matrix by  $\delta = 0.1\sigma$  (red dashed). The vector lengths are proportional to the displacements. (b) An intensity plot of the logarithm of the power spectrum  $|\vec{R}(\omega)|^2$  as a function of frequency  $\omega$  and perturbation  $\delta$  along the 6th eigenmode of the system in (a) after 170 oscillations. The solid horizontal lines indicate the 22 harmonic eigenfrequencies for (a). The inset shows the same calculation except for a two-sided linear spring potential. (c) Same as (b) except for  $N = 58$  at  $\Delta\phi = 10^{-5}$  with perturbation in mode 40 after 150 oscillations. The inset shows a close-up of the transition.

linear repulsive spring potential

$$V(r_{ij}) = \frac{\epsilon}{2} \left(1 - \frac{r_{ij}}{\sigma_{ij}}\right)^2 \Theta\left(1 - \frac{r_{ij}}{\sigma_{ij}}\right), \quad (1)$$

where  $r_{ij}$  is the center-to-center separation between disks  $i$  and  $j$ ,  $\epsilon$  is the characteristic energy scale,  $\Theta(x)$  is the

Heaviside function, and  $\sigma_{ij} = (\sigma_i + \sigma_j)/2$  is the average diameter. We have also studied systems with Hertzian and purely repulsive Lennard-Jones interactions, but the repulsive linear spring potential provides a ‘lower bound’ on the degree of nonlinearity arising from one-sided interactions. Energy, length, and timescales are measured in units of  $\epsilon$ ,  $\sigma$ , and  $\sqrt{m/\epsilon\sigma}$ , respectively.

The MS packings were generated using the compression and energy minimization protocol described in Ref. [16]. Each MS packing is characterized by a packing fraction  $\phi_J$  above which the potential energy  $V$  and pressure  $p$  of the system begins to increase from zero. The distance in packing fraction from  $\phi_J$  is tuned from  $\Delta\phi = 10^{-8}$  to  $10^{-1}$  and the positions of the particles are accurate to  $10^{-16}$  at each  $\Delta\phi$ . We calculate the eigenfrequencies  $\omega_i$  and eigenmodes  $\hat{e}_i = \{\hat{e}_i^1, \hat{e}_i^2, \dots, \hat{e}_i^N\} = \{e_{xi}^1, e_{yi}^1, e_{xi}^2, e_{yi}^2, \dots, e_{xi}^N, e_{yi}^N\}$  (with  $\hat{e}_i^2 = 1$ ) in the harmonic approximation from the dynamical matrix evaluated at the MS packing. Since the systems are mechanically stable, the  $\mathcal{N} = 2N' - 2$  eigenfrequencies  $\omega_i > 0$  [15], where  $N' = N - N_r$  and  $N_r$  is the number of rattler particles with less than three contacts per particle. We index the eigenfrequencies from smallest to largest,  $i = 1$  to  $\mathcal{N}$ , removing the two trivial eigenfrequencies corresponding to uniform translations.

To test whether the packings possess a harmonic regime, we apply displacements to individual particles and then evolve the system at constant total energy  $E$ . Specifically, at time  $t = 0$ , we apply the displacement

$$\vec{R} - \vec{R}^0 = \delta \hat{e}_i, \quad (2)$$

where the new configuration  $\vec{R} = \{\vec{R}_1, \vec{R}_2, \dots, \vec{R}_N\} = \{x_1, y_1, \dots, x_N, y_N\}$ , and  $\vec{R}^0$  is the original MS packing. We remove rattlers from the MS packings prior to applying the perturbations. A sample perturbation for  $N = 12$  along the 6th mode is shown in Fig. 1 (a). For  $t > 0$ , we solve Newton’s equations of motion at constant  $E$ , and measure the particle displacements and number of contacts as a function of the number of oscillations  $n$  for perturbations along each mode  $k$ .

**Results** In Fig. 1 (b), we show the logarithm of the power spectrum  $|\vec{R}(\omega)|^2$ , where  $\vec{R}(\omega) = \int_0^{nT_6} dt e^{i\omega t} \vec{R}(t)$  for  $n = 170$  oscillations, where  $T_6 = 2\pi/\omega_6$ , as an intensity plot versus the perturbation amplitude  $\delta$  (along the 6th mode) and  $\omega$  for the system shown in Fig. 1 (a) with linear repulsive spring interactions. This plot demonstrates several key features: (1) There is an extremely sharp onset of nonharmonicity at  $\log_{10} \delta_c/\sigma \simeq -6.8$ . For  $\delta < \delta_c^a$ , the system vibrates with  $\omega = \omega_6$ . Although  $\delta_c^a$  depends on the excitation mode, the transition for each mode is sharp. (2) For  $\delta \gtrsim \delta_c^a$ , the response spreads to include other harmonic eigenfrequencies (shown as solid horizontal lines in Fig. 1 (b)) and  $|\vec{R}(\omega)|^2 \sim \omega^{-2}$  similar to equipartition in thermal equilibrium. (3) For larger perturbations, the power spectrum develops a continuous frequency band in which the harmonic eigenfrequencies are completely lost. At sufficiently large amplitudes, the

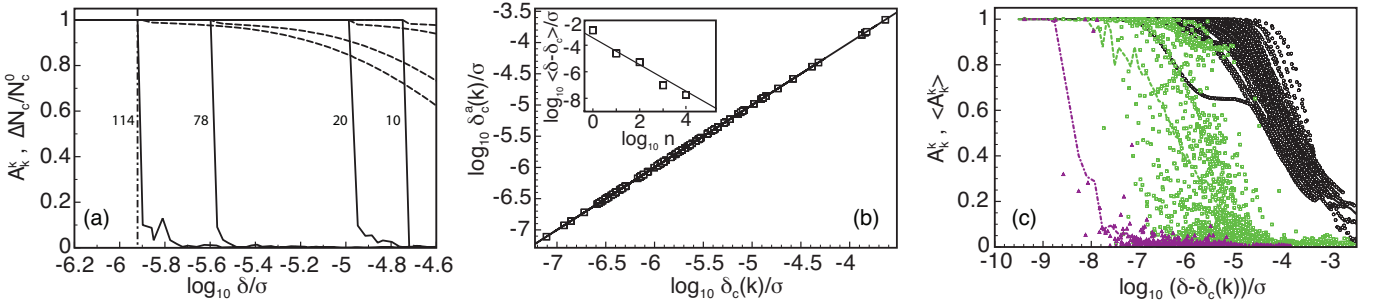


FIG. 2: (a) Amplitude  $A_k^k$  (solid) and deviation of the number of contacts  $\Delta N_c = N_c^0 - \langle N_c \rangle_t$  relative to the unperturbed number  $N_c^0$  (dashed) versus perturbation amplitude  $\delta$  along four eigenmodes (labeled by mode number) for the system in Fig. 1 (c) after  $n = 10^4$  oscillations. The vertical dot-dashed line indicates  $\delta = \delta_c^a$  for  $k = 114$ . (b) The measured  $\delta_c^a(k)$  at which  $A_k^k$  and  $\langle N_c \rangle_t$  begin to deviate from 1 for perturbations along all eigenmodes at  $n = 10^4$ ,  $N = 58$ , and  $\Delta\phi = 10^{-5}$  versus the calculated deformation amplitude  $\delta_c(k)$  in Eq. 4 at which the first contact breaks. The inset displays the values  $\delta^* - \delta_c(k)$  at which  $\langle A_k^k \rangle$  decays to 0.2 as a function of  $n$ . The solid line has slope  $-1$ . (c)  $A_k^k$  versus  $\delta - \delta_c(k)$  for each  $k$  (open symbols) and  $\langle A_k^k \rangle$  averaged over  $k$  (lines) for  $n = 1$  (circles, solid line),  $10^2$  (squares, dashed line), and  $10^4$  (triangles, dot-dashed line) oscillations after the perturbation.

dominant contribution to the broad power spectrum approaches  $\omega = 0$ . Note that this crossover to nonharmonic frequency response occurs at much larger amplitudes in systems with smooth nonlinear interaction potentials.

For larger systems the transition from harmonic to nonharmonic behavior is similar (Fig. 1 (c)). The inset to Fig. 1 (c) shows that large systems display an intermediate nonharmonic regime in which a subset of harmonic eigenmodes are populated at the onset of nonharmonicity,  $\delta = \delta_c^a$ . To put the effects of one-sided potentials into perspective, we compare these results with those from two-sided spring potentials (*i.e.* Eq. 1 with the argument of  $\Theta$  replaced by  $1 - R_{ij}/\sigma_{ij}$ ). For  $N = 12$ , the transition for systems with one-sided repulsive spring interactions occurs at perturbations more than four orders of magnitude smaller than those for systems with double-sided spring potentials [15] and the transition occurs slowly over a decade in  $\delta$  (inset to Fig. 1 (b)).

To quantify the harmonic to nonharmonic transition, we calculate the number of particle contacts  $\langle N_c \rangle_t$  averaged over time and define a harmonicity parameter  $A_k^k$  that measures the spectral content of the particle displacements in the eigenmode direction  $k$  at eigenfrequency  $\omega_k$  following a perturbation along eigenmode  $k$ :

$$A_k^k = \left| \frac{\int_0^{nT_k} \Delta \vec{R}(t) \cdot \hat{e}_k \cos(\omega_k t) dt}{\delta \int_0^{nT_k} \cos^2(\omega_k t) dt} \right|, \quad (3)$$

where  $\Delta \vec{R}(t) = \vec{R}(t) - \langle \vec{R}(t) \rangle_t$ .  $A_k^k = 1$  for harmonic systems and  $A_k^k \approx 0$  for nonharmonic systems that do not oscillate in mode  $k$  at  $\omega_k$ . We also calculate the harmonicity parameter  $\langle A_k^k \rangle$  averaged over all individually perturbed modes  $k$ .

In Fig. 2 (a), we plot  $A_k^k$  and the deviation in the time-averaged number of contacts  $\Delta N_c = N_c^0 - \langle N_c \rangle_t$  relative to the unperturbed value  $N_c^0$  versus  $\delta$  along several modes  $k$  for the system in Fig. 1 (c). We find that  $A_k^k$  for each mode  $k$  begins to decrease from 1 at the same  $\delta_c^a(k)$  where the average number of contacts  $\langle N_c \rangle_t$  begins to

deviate from  $N_c^0$ . For perturbations along each mode  $k$ , the transition from harmonic to nonharmonic behavior occurs when a *single* existing contact breaks. To verify this, we plot in Fig. 2 (b)  $\delta_c^a(k)$  versus the predicted amplitude  $\delta_c(k)$  at which the first contact breaks. The predicted value  $\delta_c(k)$  is obtained by solving  $R_{ij}^2 = \sigma_{ij}^2$  for all contacting pairs of particles  $i$  and  $j$  for a given MS packing and perturbation along mode  $k$ , and identifying the minimum  $\delta_c(k) = \min_{ij} |\delta_{ij}(k)|$ , where

$$\delta_{ij}(k) = \frac{|\vec{e}_k^{ij} \cdot \vec{R}_{ij}^0|}{|\vec{e}_k^{ij}|^2} \left( \sqrt{1 + \frac{(\sigma_{ij}^2 - |\vec{R}_{ij}^0|^2)|\vec{e}_k^{ij}|^2}{|\vec{e}_k^{ij} \cdot \vec{R}_{ij}^0|^2}} - 1 \right). \quad (4)$$

We find that the  $\delta$  at which  $A_k^k$  begins to decrease,  $\delta_c^a(k) = \delta_c(k)$  at which a single contact breaks (as shown in Fig. 2 (b)) over a wide range of  $\Delta\phi$  and  $N$  with a relative error less than  $10^{-3}$  over four orders of magnitude in  $\delta_c(k)$ . For larger system sizes, it is possible that new contacts can form before existing contacts break, but we find that this does not occur for the system sizes and compressions studied.

The rate at which energy input via a perturbation along eigenmode  $k$  is transferred out of that mode and into other displacement modes determines the shape of the decay of  $A_k^k$ . In Fig. 2 (c), we show  $A_k^k$  and  $\langle A_k^k \rangle$  versus  $\delta - \delta_c(k)$  for  $n = 1$ ,  $10^2$ , and  $10^4$  oscillations for perturbations along each mode  $k$  individually. For small  $n$ , even though  $A_k^k$  begins to decrease from 1 at  $\delta_c(k)$ , the shape of the decay depends on  $k$  and the sharp decrease from 1 to 0 occurs at small but finite  $\delta - \delta_c(k)$ . In the inset to Fig. 2 (b), we measure the amplitude  $\delta^* - \delta_c(k)$  at which  $\langle A_k^k \rangle$  decays to a small value (0.2), and find  $\delta^* - \delta_c(k) \sim 1/n$ . For all  $n$  and perturbations  $\delta$  studied in Fig. 2, there is no detectable nonharmonicity from the smooth nonlinearities in the potential [15] in Eq. 1.

Thus,  $\delta_c(k)$  is the critical deformation amplitude above which MS packings become nonharmonic, and  $\delta_c(k)$  can be calculated exactly using Eq. 4 for each MS packing

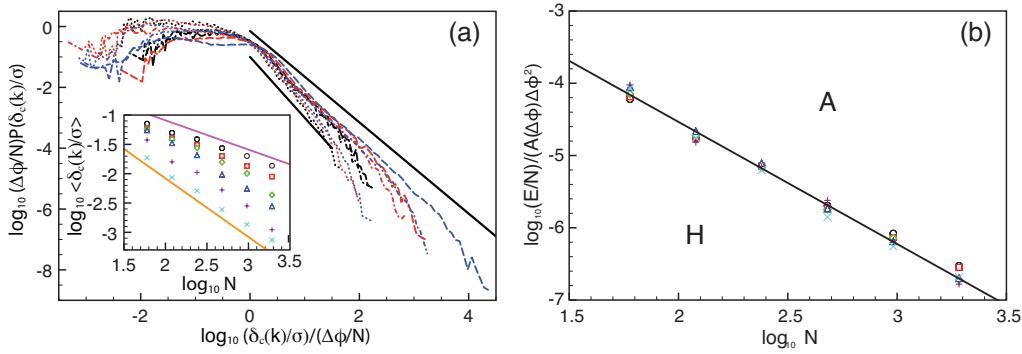


FIG. 3: (a) Distribution  $P(\delta_c(k))$  (scaled by  $\Delta\phi/N$ ) versus  $\delta_c(k)N/\Delta\phi$  for  $\Delta\phi = 10^{-2}$  (dotted),  $10^{-4}$  (dot-dashed), and  $10^{-7}$  (dashed) and  $N = 60$  (black),  $240$  (red), and  $1920$  (blue). The two solid black lines have slope  $1.5$  and  $2$ . The inset shows the scaling of  $\langle\delta_c(k)\rangle$  with  $N$  for  $\Delta\phi = 10^{-2}$  (crosses),  $10^{-3}$  (pluses),  $10^{-4}$  (upward triangles),  $10^{-5}$  (diamonds),  $10^{-6}$  (squares), and  $10^{-7}$  (circles). The two solid lines have slope  $1$  and  $0.5$ . (b) The total energy per particle required to break a single contact averaged over  $k$  (scaled by  $A(\Delta\phi)(\Delta\phi)^2$ ) versus system size  $N$  for  $\Delta\phi = 10^{-2}$  (crosses),  $10^{-3}$  (pluses),  $10^{-4}$  (upward triangles),  $10^{-5}$  (diamonds),  $10^{-6}$  (squares), and  $10^{-7}$  (circles). The solid line has slope  $-1.7$ .

and mode  $k$ . In Fig. 3 (a) we show the distribution  $P(\delta_c(k)/\sigma)$  of critical amplitudes with the vertical and horizontal axes scaled by  $\Delta\phi/N$  to achieve approximate collapse. We find that the distribution  $P(\delta_c(k)/\sigma)$  scales roughly as a power law  $(\delta_c(k)/\sigma)^\alpha$  for large  $\delta_c$  with  $\alpha \approx 2$  ( $1.5$ ) for large (small)  $\Delta\phi$ . The distribution is cut-off and remains nearly constant for  $\delta_c(k)/\sigma < \Delta\phi/N$ . In the inset to Fig. 3 (a), we plot  $\langle\delta_c(k)\rangle$  averaged over  $k$  versus  $N$  over a range of  $\Delta\phi = 10^{-7}$  to  $10^{-2}$ . As expected from the power-law distribution in the main plot,  $\langle\delta_c(k)\rangle \sim N^{\alpha-1}$ . For all  $\Delta\phi$ , the critical deformation amplitude scales to zero in the large system limit.

The potential energy  $V$  of a MS packing prepared at  $\Delta\phi$  is given by  $V/N = B(\Delta\phi)^2$  [6], where  $B$  is a  $O(1)$  constant. We find that the average deformation energy  $E^* \approx \langle(\omega_k \delta_c(k))^2\rangle$  for the critical amplitude scales as  $E^* \sim A(\Delta\phi)(\Delta\phi)^2/N^\beta$ , where  $A(\Delta\phi)$  is only weakly dependent on  $\Delta\phi$  and  $\beta \approx 1.7$ . For  $E > E^*$  (labeled  $A$  in

Fig. 3 (b)), MS packings are strongly anharmonic. MS packings are only harmonic for  $E < E^*$ , where  $E^* \rightarrow 0$  in the large system limit for all  $\Delta\phi$ . Thus, eigenfrequencies of the dynamical matrix do not describe vibrations of MS packings as  $N \rightarrow \infty$  for all  $\Delta\phi$ .

**Conclusion** We have shown that one-sided repulsive interactions in jammed particulate systems make them inherently nonharmonic. In the large system limit at any compression and in the  $\Delta\phi \rightarrow 0$  limit at any system size, infinitesimal perturbations will cause them to become strongly nonharmonic, which will affect their mechanical response, specific heat, and energy diffusivity. In future studies, we will explore the possibility of defining dynamic steady-state packings with robust effective harmonic modes obtained from average particle positions.

**Acknowledgments** This research was supported by the National Science Foundation under Grant Nos. DMS-0835742 (CO, TB, CS) and CBET-0968013 (MS).

- 
- [1] J. A. TenCate, D. Pasqualini, S. Habib, K. Heitmann, D. Higdon, and P. A. Johnson, Phys. Rev. Lett. **93** (2004) 065501.
  - [2] X. Jacob, V. Aleshin, V. Tournat, P. Leclaire, W. Lauriks, and V. E. Gusev, Phys. Rev. Lett. **100** (2008) 158003.
  - [3] C.-h. Liu and S. R. Nagel, Phys. Rev. B **48** (1993) 15646.
  - [4] O. Mouraille, W. A. Mulder, and S. Luding, J. Stat. Mech. **2006** (2006) P07023.
  - [5] H. A. Makse, N. Gland, D. L. Johnson, and L. Schwartz, Phys. Rev. E **70** (2004) 061302.
  - [6] C. S. O'Hern, L. E. Silbert, A. J. Liu, and S. R. Nagel, Phys. Rev. E **68** (2003) 011306.
  - [7] L. E. Silbert, A. J. Liu, and S. R. Nagel, Phys. Rev. Lett. **95** (2005) 098301.
  - [8] K. Chen, W. G. Ellenbroek, Z. Zhang, D. T. N. Chen, P. J. Yunker, S. Henkes, C. Brito, O. Dauchot, W. van Saarloos, A. J. Liu, and A. G. Yodh, Phys. Rev. Lett. **105** (2010) 025501.
  - [9] V. Vitelli, N. Xu, M. Wyart, A. J. Liu, and S. R. Nagel, Phys. Rev. E **81** (2010) 021301.
  - [10] K. L. Johnson, *Contact Mechanics* (Cambridge University Press, Cambridge, England, 1985)
  - [11] C.-h. Liu, S. R. Nagel, D. A. Schecter, S. N. Coppersmith, S. Majumdar, O. Narayan, and T. A. Witten, Science **269** (1995) 513.
  - [12] E. T. Owens and K. E. Daniels, "The effect of force chains on granular acoustics," preprint (2010).
  - [13] V. Tournat, V. E. Gusev, and B. Castagnede, Phys. Lett. A **326** (2004) 340.
  - [14] A. Tanguy, J. P. Wittmer, F. Leonforte, and J.-L. Barrat, Phys. Rev. B **66** (2002) 174205.
  - [15] See supplementary material at <http://link.aps.org/supplemental/>.
  - [16] G.-J. Gao, J. Blawdziewicz, and C. S. O'Hern, Phys. Rev. E **74** (2006) 061304.
  - [17] L. E. Silbert, A. J. Liu, and S. R. Nagel, Phys. Rev. E **73** (2006) 041304.
  - [18] A. Donev, S. Torquato, and F. H. Stillinger, Phys. Rev. E **71** (2005) 011105.